Fig. 3. Slow-wave factors versus frequency for modified CPS with 3 different outer slot widths and conventional CPS (substrate: $\epsilon_R = 9.9$, thickness: 25 mil).

TABLE I
CPS DIMENSIONS

	Case a	Case b	Case c	Case d
Inner slot width (mm)	.635	.635	.635	.635
Conductor width (mm)	.635	.635	.635	.635
Outer slot width (mm)	∞	1.27	.635	.3125

TABLE II
COMPARISON OF SLOW WAVE FACTORS CALCULATED BY QUASI-STATIC AND FULL WAVE ANALYSES

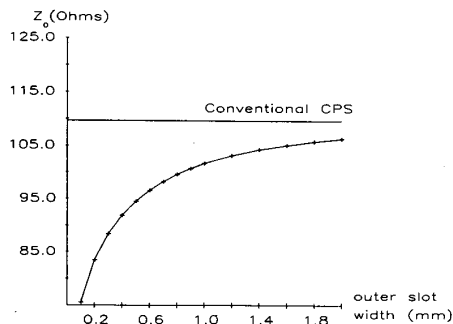|	Case b	Case c	Case d
Quasi-static value	2.12	2.16	2.20
Fullwave Analysis (5 GHz)	2.13	2.19	2.23

Fig. 4. Variation with outer slot width of the characteristic impedance of modified CPS. (Inner slot width: .635 mm, substrate thickness: .635 mm, ϵ_R: 9.9)

quasi-static values of the propagation constant and characteristic impedance reduce to those given for conventional CPS [7]. While it is not completely consistent, it may be more accurate to replace ϵ_{eff} in the quasi-static expression for characteristic impedance with the value of ϵ_{eff} calculated using the spectral domain approach as was done in [8].

CONCLUSION

A new configuration of coplanar stripline has been proposed and analyzed using both quasi-static and fullwave analysis. The modified configuration offers several advantages over conventional CPS. First, line to line coupling is reduced because of the isolation provided by the ground planes. Second, the parasitic TE_0 dielectric slab waveguide mode, which plagues conventional CPS, is eliminated. Finally, flexibility in obtaining lower characteristic impedances is added by the possibility of adjusting the outer slot width. This configuration of CPS should be useful in the realization of balanced lines with high isolation.

REFERENCES

[1] R. A. Pucel, "Design considerations for monolithic microwave circuits," IEEE Trans. Microwave Theory Tech., vol. MTT-29, no. 6, June 1981.
[2] D. B. Rutledge, D. P. Neikirk, and D. P. Kasilinganm, "Integrated circuit antennas," in Infrared and Millimeter Waves, vol. 10, Millimeter Components and Techniques, Part II, Kenneth J. Button, Ed., Orlando, FL: Academic Press, 1983.
[3] J. S. McLean, A. D. Wieck, K. Ploog, and T. Itoh, "Full Wave Analysis of Open-end Discontinuities in Coplanar Stripline and Finite Ground Plane Coplanar Waveguide," in Proc. 21st European Microwave Conf., Sept. 9–12, 1991.
[4] G. Ghione and C. V. Naldi, "Coplanar waveguides for MMIC applications: Effect of upper shields, conductor backing, finite-extent ground planes, and line to line coupling," IEEE Trans. Microwave Theory Tech., vol. MTT-35, no. 3, Mar. 1987.
[5] T. Itoh, Numerical Techniques for Microwave and Millimeter-wave Passive Structures. New York: Wiley, 1989.
[6] J. B. Knorr and K. Kuchler, "Analysis of coupled slots and coplanar strips on dielectric substrate," IEEE Trans. Microwave Theory Tech., vol. MTT-23, no. 7, pp. 541–548, July 1975.
[7] G. Ghione and C. Nalde, "Analytical formulas for coplanar lines in hybrid and monolithic MICs," Electron. Lett., vol. 20, no. 4, pp. 179–181, February 16, 1984.
[8] Y. C. Shih and T. Itoh, "Analysis of conductor-backed coplanar waveguide," Electron. Lett., vol. 18, no. 12, pp. 538–540, June 10, 1982.

A Dispersive Boundary Condition for Microstrip Component Analysis Using The FD-TD Method

Zhiqiang Bi, Keli Wu, Chen Wu, and John Litva

Abstract—A dispersive absorbing boundary condition (DBC) is presented, which allows the dispersion characteristics of waves to be used as a criterion for designing absorbing boundary conditions. Its absorbing quality is superior to that of the presently used Mur's first order boundary condition for microstrip component analysis, and, as well, its implementation is much simpler when compared to that of the "super boundary condition" treatment. Due to the significant performance improvement of the new boundary condition, the memory requirement can be reduced greatly when applying this boundary condition to microstrip component analysis.

I. INTRODUCTION

Recently, FD-TD methods have been used to calculate the frequency-dependent characteristic of microstrip discontinuities [1]–[3], microstrip components and simple microstrip antennas [4] and complex microstrip antennas [5], [6]. All of these calculations have shown the FD-TD method to be a very powerful tool for microstrip component and antenna analysis because it has the following two desirable attributes. First, it can be applied to problems exhibiting a complex structure which may be very difficult to solve using other analytical or numerical methods. Second, only one computation is required to get the frequency domain results over a large frequency spectrum. However, this method has one significant drawback, which is that it requires very large computer memories, even for the analysis of very simple microstrip lines and coplanar waveguides [1]–[3]. One of the first approaches to be tried for reducing the memory requirement is to use a good absorbing boundary condition so that a smaller computational domain can be used. The authors of earlier papers have used the one dimensional absorbing boundary condition or Mur's first order absorbing boundary condition (ABC), which is not accurate enough for microstrip analysis, especially for high dielectric constant microstrip components. The reason for this is tied to the fact that, when a gaussian pulse travels on the microstrip line, the velocities of fields are different for different frequencies due to the dispersion property of microstrip line or coplanar line. When applying Mur's first-order ABC it is found that it falls short of the mark because it is an effective absorber of waves at only one phase velocity or one frequency.

The purpose of this paper is to investigate a dispersive boundary condition (DBC) which can absorb waves over a wide frequency band. The performance of this DBC is much better than that of the presently used Mur's first order boundary condition [2]–[4], and its implementation is much easier compared with that of "super boundary condition" treatment of [2] and [3]. The significant improvement in performance of the present DBC compared with others will be demonstrated with the numerical analysis of a microstrip line.

II. DISPERSIVE BOUNDARY CONDITION (DBC)

In most FD-TD analysis of microstrip components, such as microstrip lines, basic microstrip discontinuities and microstrip antennas, the major direction of the power flow is in the waveguided direction (for a microstrip line, in the metal strip direction). The sideways leakage and radiation are small due to the guiding nature of the metal strip and the high-dielectric constant of the substrate. This is quite similar to the one dimensional propagation case. Based on the above observation, papers [2]–[4] use the following one dimensional boundary condition or Mur's first order boundary condition:

$$\left(\frac{\partial}{\partial z} + \frac{1}{v_i}\frac{\partial}{\partial t}\right) E = 0 \tag{1}$$

where E represents the tangential electric field component relative to the boundary wall and v_i represents the velocity of propagation of the fields. Since the above boundary condition can only be optimized for a wave whose frequency corresponds to the velocity, v_i, the magnitude of the energy reflected by the boundary can be quite large due to reflections at other frequencies. Here, we present a dispersive boundary condition which can absorb fields over a wide frequency band.

It can be proved that the following boundary condition can ab-

sorb plane waves traveling to the right with velocities v_1 and v_2:

$$\left(\frac{\partial}{\partial z} + \frac{1}{v_1}\frac{\partial}{\partial t}\right)\left(\frac{\partial}{\partial z} + \frac{1}{v_2}\frac{\partial}{\partial t}\right) E = 0. \tag{2}$$

This is because if $E = E(z - vt)$ is a plane wave traveling with velocity v, then

$$\left(\frac{\partial}{\partial z} + \frac{1}{v_1}\frac{\partial}{\partial t}\right)\left(\frac{\partial}{\partial z} + \frac{1}{v_2}\frac{\partial}{\partial t}\right) E$$

$$= \left(\frac{\partial}{\partial z} + \frac{1}{v_1}\frac{\partial}{\partial t}\right)\left(E' - \frac{v}{v_2}E'\right)$$

$$= E'' - \frac{v}{v_2}E'' - \frac{v}{v_1}E'' + \frac{v^2}{v_1 v_2}E''$$

$$= \frac{1}{v_1 v_2}(v_2 - v)(v_1 - v)E''. \tag{3}$$

Therefore the above equation is equal to zero if v is equal to one of the velocities. So, the boundary condition (2) can absorb any linear combination of plane waves propagating with velocities v_1 and v_2. By concatenating several absorbing boundary conditions (1), the number of the absorption velocities can be increased. A dispersive wave can be decomposed into many different frequency components. Each frequency component corresponds to a plane wave with velocity v, which is determined by the dispersion relation:

$$v = v(f) \tag{4}$$

where f is the frequency and $v(f)$ is any form of function which depends on the analyzed structures. So, if v_1 and v_2 are determined by the dispersion relation $v = v(f)$, boundary condition (2) becomes a multifrequency absorbing boundary condition or a dispersive boundary condition (DBC).

Actually, Keys and Higdon's angle absorbing boundary condition [7]–[9] can also be described in terms of (2). In their work, they choose the velocity v according to the relation $v_i = c/\cos\theta_i$, where c is the propagation velocity of wave, and θ_i is the incident angle of the wave with respect to the z-axis. The reason they can make this choice for the phase velocity is due to the following fact: A plane wave with velocity c and angle θ can be expressed as

$$E(t, z) = E(ct - z\cos\theta) = E\left(\frac{c}{\cos\theta}t - z\right) \tag{5}$$

along the z-axis. Moreover, an arbitrary wave can be decomposed into a summation of plane waves with different angles, i.e.:

$$E(t, z) = \sum_i E_i(ct - z\cos\theta_i) = \sum_i E_i\left(\frac{c}{\cos\theta_i}t - z\right). \tag{6}$$

The implementation of the dispersive boundary (2) can be realized by employing operators. Let us define the shift operators I, Z and K_z by the following:

$$IE_i^n = E_i^n \tag{7}$$

$$ZE_i^n = E_i^{n+1} \tag{8}$$

$$K_z E_i^n = E_{i+1}^n \tag{9}$$

where i is the space position index and n is the time index. The difference equation of (1) is

$$E_M^n - E_{M-1}^{n-1} - \gamma_i(E_M^{n-1} - E_{M-1}^n) = 0 \tag{10}$$

where

$$\gamma_i = \frac{1 - \rho_i}{1 + \rho_i} \tag{11}$$

$$\rho_i = \frac{v(f_i)\,\Delta t}{\Delta z} \tag{12}$$

and E_M represents the tangential electric field component on the boundary and E_{M-1} represents the tangential electric field component a distance of one node inside the boundary. The boundary condition (10) can be expressed by the operators:

$$[I - Z^{-1}K_z^{-1} - \gamma_i(Z^{-1} - K_z^{-1})]E_M^n = 0 \tag{13}$$

or

$$B_i E_M^n = 0 \tag{14}$$

where,

$$B_i = I - Z^{-1}K_z^{-1} - \gamma_i(Z^{-1} - K_z^{-1}) \tag{15}$$

is defined as the difference boundary operator. The difference boundary operator B for the dispersive boundary condition given by (2) can be obtained in the following way:

$$B = B_1 B_2$$

$$= [I - Z^{-1}K_z^{-1} - \gamma_1(Z^{-1} - K_z^{-1})]$$

$$\cdot [I - Z^{-1}K_z^{-1} - \gamma_2(Z^{-1} - K_z^{-1})]$$

$$= I - 2Z^{-1}K_z^{-1} + Z^{-2}K_z^{-2} + \gamma_1\gamma_2(Z^{-2} - 2Z^{-1}K_z^{-1} + K_z^{-2})$$

$$- (\gamma_1 + \gamma_2)(Z^{-1} - K_z^{-1} - Z^{-2}K_z^{-1} + Z^{-1}K_z^{-2}). \tag{16}$$

From the above boundary operator, we can get the final second-order dispersive boundary condition:

$$E_M^n = 2E_{M-1}^{n-1} - E_{M-2}^{n-2}$$

$$+ (\gamma_1 + \gamma_2)(E_M^{n-1} - E_{M-1}^n - E_{M-1}^{n-2} + E_{M-2}^{n-1})$$

$$- \gamma_1\gamma_2(E_M^{n-2} - 2E_{M-1}^{n-1} + E_{M-2}^n). \tag{17}$$

III. NUMERICAL RESULTS

Using the above dispersive boundary condition, we carry out an analysis on a mictrostrip line. Fig. 1 gives the effective dielectric constant calculated using the FD-TD method. The analysis is carried out by applying both the dispersive boundary condition and Mur's first-order boundary at the end of the microstrip line, while at the other walls we only use Mur's first-order boundary condition. The curve identified by crosses was obtained by using a computation domain which is as large as that used in [1] so that the time domain data can be truncated before reflections from the boundary occur. This is an exact result in the sense that it is free of any boundary effects. The curve idenitifed by circles was obtained by using the DBC and using only one third of the former computation domain. In the DBC, the velocities v_1 and v_2 were determined by using values 7.12 and 8.50, respectively, for the effective dielectric constant. The above two lines overlap exactly in this figure. The dashed line results from using Mur's first order ABC and the smaller computation domain. In Mur's first-order ABC, the velocity is determined by using an effective dielectric constant of 7.12. This result shows that by using the DBC, the computation memory requirement can be reduced greatly. In Fig. 2 is shown a propagating E_x-pulse in the time domain, as well as a residual signal due to reflections at the boundary of the computa-
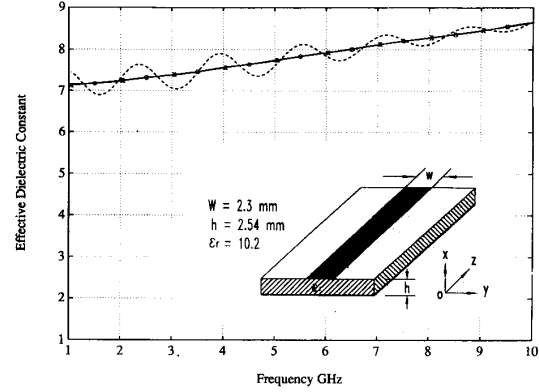

Fig. 1. Effective dielectric constant of a microstrip line. The cross dotted line: Using very large computation domain. The circular dotted line: Using DBC and smaller computation domain. The dashed line: Using Mur's first order ABC and smaller computation domain.
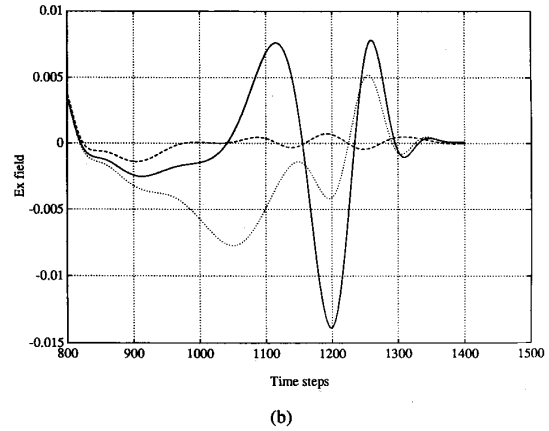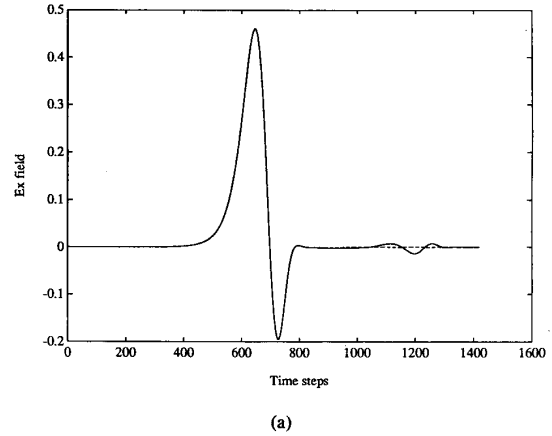

(a)

(b)

Fig. 2. Field reflection in time domain due to boundary conditions. (a) Incident waves and reflected waves from the boundary conditions. Solid line: first order ABC, $\epsilon_{reff} = 7.12$ Dashed line: DBC, $\epsilon_{reff\,1} = 7.12$, $\epsilon_{reff\,2} = 8.50$ (b) Reflected waves from the boundary conditions. Solid line: first order ABC, $\epsilon_{reff} = 7.12$. Dotted line: first order ABC, $\epsilon_{reff} = 8.12$. Dashed line: DBC, $\epsilon_{reff\,1} = 7.12$, $\epsilon_{reff\,2} = 8.50$.
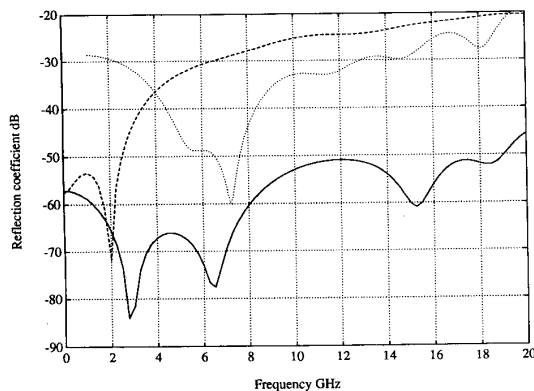
Fig. 3. Numerical experiment reflection coefficient for a microstrip line. Solid line: first order ABC, $\epsilon_{reff} = 7.12$. Dotted line: first order ABC, $\epsilon_{reff} = 8.12$. Dashed line: DBC, $\epsilon_{reff1} = 7.12$, $\epsilon_{reff2} = 8.50$.

tion domain for both DBC and Mur's boundary condition. In the DBC, $\epsilon_{reff1} = 7.12$ and $\epsilon_{reff2} = 8.50$ are used to determine the two velocities. In Mur's first-order ABC, $\epsilon_{reff} = 7.12$, 8.12 are used to determine the velocity, respectively. From this result we see that in the time domain the reflections from the computation domain boundary are greatly reduced using DBC: in fact, DBC reflections are an order of magnitude less than those from the first-order boundary conditions. The numerical reflection coefficients for both DBC and the first-order boundary conditions are given in Fig. 3. This figure shows that DBC absorbs the wave over a large frequency band, i.e., the reflection coefficient is less than −45 dB from 0 to 20 GHz, where $\epsilon_{reff1} = 7.12$ and $\epsilon_{reff2} = 8.50$ are used for the DBC. For the first-order condition, the reflection coefficients are less than −45 dB only over the ranges from 0 to 3 GHz when $\epsilon_{reff} = 7.12$, or from 5 to 8 GHz when $\epsilon_{reff} = 8.12$.

IV. CONCLUSION

The dispersive boundary condition allows the dispersion of waves to be incorporated into the design of an absorbing boundary condition. This feature can be very useful when the dispersion for a major outgoing wave is known. Both the validity and the efficiency of the DBC have been demonstrated by carrying out analyses on a microstrip line. With DBS, the memory requirement for FD-TD analyses of microstrip components and antennas can be greatly reduced.

The main difference between DBC and ABC is that DBC is designed to optimize the boundary condition according to the dispersion characteristics of waves, while ABC is designed to optimize the boundary condition according to the propagation direction of the waves. The introduction of the concepts which are the basis of DBC is specially important for study of absorption for strongly dispersive waves, such as occurs in conductor waveguides and dielectric waveguides. The further application of the proposed DBC to waveguide component analysis has been investigated in a separate paper [10]. Based on the ideas presented in this paper, some ABC's can be modified into DBC's.

REFERENCES

[1] X. Zhang, J. Fang, K. K. Mei, and Y. Liu, "Calculations of the dispersive characteristics of microstrips by the time-domain finite-dif-

ferent method," *IEEE Trans. Microwave Theory Tech.*, vol. 36, pp. 263–267, Feb. 1988.
[2] X. Zhang and K. K. Mei, "Time domain finite difference approach to the calculation of the frequency dependent characteristics of microstrip discontinuities," *IEEE Trans. Microwave Theory Tech.*, vol. 36, pp. 1775–1787, Dec. 1988.
[3] G. Liang, Y. Liu, and K. K. Mei, "Full-wave analysis of coplanar waveguide and slotline using the time-domain finite-difference method," *IEEE Trans. Microwave Theory Tech.*, vol. 37, pp. 1949–1957, Dec. 1989.
[4] D. M. Sheen, S. M. Ali, M. D. Abouzahra, and J. A. Kong, "Application of the three-dimensional finite-difference time-domain method to the analysis of planar microstrip circuits," *IEEE Trans. Microwave Theory Tech.*, vol. 38, pp. 849–857, July 1990.
[5] J. Litva, Z. Bi, K. Wu, R. Fralich, and C. Wu, "Full-wave analysis of an assortment of printed antenna structures using the FD-TD method," *1991 IEEE AP-S Int. Symp. Dig.*, June 1991, pp. 410–413.
[6] C. Wu, K. Wu, Z. Bi, and J. Litva, "Accurate Characterization of planar printed antennas using finite difference time domain method," submitted to *IEEE Trans. Antennas Propagat.*
[7] R. G. Keys, "Absorbing boundary conditions for acoustic media," *Geophysics*, vol. 50, no. 6, pp. 892–902, July 1985.
[8] R. L. Higdon, "Numerical absorbing boundary conditions for the wave equation," *Math. Comput.*, vol. 49, no. 179, pp. 65–91, July 1987.
[9] R. L. Higdon, "Absorbing boundary conditions for difference approximations to the multi-dimensional wave equation," *Math. Comput.*, vol. 47, no. 176, pp. 437–459, Oct. 1986.
[10] Z. Bi, J. Litva, K. Wu, and C. Wu, "Dispersive absorbing boundary conditions (DBC) for waveguide component analysis using the FD-TD method," submitted to *IEEE Trans. Microwave Theory Tech.*

New Broadband Rectangular Waveguide with L-Shaped Septa

Pradip Kumar Saha and Debatosh Guha

Abstract—Rectangular waveguides with double L-shaped septa—variants of Double T-Septa Guides (DTSG) [1], [2]—have been analyzed theoretically and are proposed as new broadband waveguides. Results indicate that significant improvement in cutoff wavelength and bandwidth in particular should be available with L-shaped septa in antisymmetric configuration.

I. INTRODUCTION

Recently rectangular waveguides with T-shaped septa have been proposed as alternative to ridged waveguides [1], [2]. Theoretical analysis using the Ritz–Galerkin technique showed that the lowest TE mode of such a guide has superior cutoff, bandwidth and impedance characteristics. It was further shown theoretically that dielectric loading of the septa-gap can improve the cutoff and bandwidth significantly [3]. Experimental verification of these properties and formulations of the problems by other methods have been reported in the literature [4]–[8].

In this paper we propose another type of broadband septum waveguides—a variant of the previously reported Double T-Septa Guide (DTSG) [1]. These guides have L-shaped septa located an-